DOI:10.1021/jf101937x

Metabolic Fate of [^{14}C]Diuron and [^{14}C]Linuron in Wheat (*Triticum aestivum*) and Radish (*Raphanus sativus*)

Sophie Pascal-Lorber,* Haifaa Alsayeda, Isabelle Jouanin, Laurent Debrauwer, Cecile Canlet, and François Laurent

INRA, UMR1089 Xénobiotiques, 180 Chemin de Tournefeuille, F-31000 Toulouse, France

Metabolism of xenobiotics in plants usually occurs in three phases, phase I (primary metabolism), phase II (conjugation processes), and phase III (storage). The uptake and metabolism of [^{14}C]diuron and [^{14}C]linuron were investigated in wheat and radish. Seeds were sown in quartz sand and irrigated with a nutrient solution of either radioactive herbicide. Plants were harvested after two weeks, and metabolites were extracted and then analyzed by radio-reverse-high-performance liquid chromatography (HPLC). Uptake of the two molecules was higher in radish compared to wheat. Translocation of parent compounds and related metabolites from roots to aerial plant parts was important, especially for radish. A large proportion of extractable residues were found in radish whereas nonextractable residues amounted to 30% in wheat, mainly associated with roots. Chemical structure of metabolites was thereafter identified by acid, alkaline, and enzymatic hydrolyses followed by electrospray ionization mass spectrometry (ESI-MS) and proton nuclear magnetic resonance spectroscopy (^{1}H NMR). This study highlighted the presence of diuron and linuron metabolites conjugated to sugars in addition to N-demethylation and N-demethoxylation products.

KEYWORDS: Phenylurea herbicides; edible plants; plant uptake; metabolization; glucosylated conjugates

INTRODUCTION

Linuron, 3-(3,4-dichlorophenyl)-1-methoxy-1-methylurea, and diuron, 3-(3,4-dichlorophenyl)-1,1-dimethylurea, are herbicides belonging to the substituted phenylurea family employed in the conventional production of cereals, vegetables and fruits. Diuron is also used for weed control in noncrop areas like railway lines, parks, roads, and pavements and as an antifouling paint biocide (*1*). Phenylurea herbicides enter plants through the roots and move apoplastically with the transpiration stream to the aerial parts blocking the Hill reaction during photosynthesis. They compete with plastoquinone for binding to the D1 quinone-binding protein in the thylakoid membrane of plastids (*2*).

Linuron and diuron are relatively persistent since they exhibit DT_{50} values in soils between one month and one year, depending on soil characteristics (*3*, *4*). Due to runoff and leaching, they are detected in soils, surface water, groundwater, and sediments together with their metabolites (*5*) and could thus contaminate terrestrial and aquatic food chains. Groundwater contamination by these herbicides will still persist despite their progressive suppression (*6*). Diuron is toxic for some nontarget aquatic organisms (*7*, *8*), and the toxicity potential at cellular and subcellular levels has been indicated (*9*). Linuron is suspected to act as an androgen receptor antagonist disrupting the male reproductive system (*10*) and has been classified as a possible carcinogen in humans by the U.S. EPA (http://www.epa.gov/superfund/programs/clp/target.htm). These compounds are thus of environmental and human health concerns, and particularly their metabolites, 3,4-dichloroaniline and to a lesser extent 3-(3,4-dichlorophenyl)-1-methylurea and 3-(3,4-dichlorophenyl)urea (*11*). Main degradation pathways are N-demethylation for diuron and N-demethylation and N-demethoxylation for linuron. The involvement of cytochrome P-450 monooxygenases has been demonstrated in the metabolism of phenylurea herbicides leading to hydroxymethyl intermediates (*12*). Bacterial degradation results in the formation of 3-(3,4-dichlorophenyl)-1-methylurea and 3,4-dichloroaniline that exhibit greater toxicological effects than those of the parent compounds. However, these metabolites can sometimes be further completely mineralized (*13*, *14*). In mammals, 3-(3,4-dichlorophenyl)-1-methoxyurea, 3-(3,4-dichlorophenyl)urea and 3-(6-hydroxy-3,4-dichlorophenyl)urea were identified as major metabolites of linuron and are excreted in the urine as glucuronide or sulfate conjugates (*15*). In plants, phase I metabolites of linuron and diuron are well-known. Frear et al. (*16*) have first isolated a microsomal oxidase able to demethylate substituted 3-(phenyl)-1,1-dimethylurea substrates from leaves of cotton, plantain, buckwheat, and broadbeans. N-Demethylation products of diuron leading to 3,4-dichloroaniline were detected in spinach (*17*). However, phase II metabolites, particularly glycosyl conjugates, are less described. Formation of glycosides varies widely among plants (*18*−*20*). For natural phenolics, the nature of the conjugates—glycoside structure, number of sugar molecules—to which humans are exposed governs the bioavailability in food chains (*21*−*23*). Glycoside conjugates of xenobiotics could act in the same way.

In this context, the uptake and metabolic fate of radiolabeled [^{14}C]diuron and [^{14}C]linuron were investigated in a liliopsidae (monocotyledonous, wheat) and a magnoliopsidae (dicotyledonous, radish). To get better insight into plant metabolism, tobacco cell

*Corresponding author. Tel: +33 561.28.53.92. Fax: +33 561.28.52.44. E-mail: spascal@toulouse.inra.fr.

cultures were also used. Structure of metabolites was determined by MS and NMR after radio-reverse-HPLC analysis. In parallel, the distribution of radioactivity between extractable and nonextractable residues and the translocation of parent compounds and related metabolites from roots to aerial parts were measured. Our study clearly evidenced new sugar conjugated metabolites of diuron and linuron.

MATERIALS AND METHODS

Chemicals. [U-phenyl-^{14}C]Linuron (specific activity 1.92×10^9 Bq mmol^{-1}, radiochemical purity >98% as determined by radio-RP-HPLC analysis) was purchased from Izotop (Budapest, Hungary). [^{14}C]-3,4-Dichloroanilin (specific activity 3.7×10^8 to 1.11×10^9 Bq mmol^{-1}, radiochemical purity >97% as determined by radio-RP-HPLC analysis), linuron (98% pure), diuron (97% pure), almond β-glucosidase (G-0395), rabbit liver esterase (E-9636), potassium phosphate, sucrose, myoinositol, thiamine, and 2,4-dichlorophenoxyacetic acid were purchased from Sigma-Aldrich (Saint-Quentin-Fallavier, France). 3,4-Dichloroanilin (97% pure), pyridine, and dimethylcarbamoyl chloride were obtained from Fluka (Saint-Quentin-Fallavier, France). Sodium acetate and sodium hydroxide were purchased from VWR International (Fontenay-sous-Bois, France). Solvents used for extractions and radio-HPLC analyses were obtained from Scharlau Chemie (Barcelona, Spain). Unless otherwise specified, all other chemicals were of analytical grade. Standards, 3-(3,4-dichlorophenyl)urea (98% pure) and 3-(3,4-dichlorophenyl)-1-methylurea (99% pure) were supplied by Dr. Ehrenstorfer GmbH (Augsburg, Germany).

Synthesis of [^{14}C]Diuron. Non-radiolabeled 3,4-dichloroanilin (0.05 mmol) in 80 μL of ethanol and 2.96×10^6 Bq of [U-phenyl-^{14}C]-3,4-dichloroanilin were mixed. Ethanol was thereafter evaporated under nitrogen. Pyridine (200 μL) and dimethylcarbamoyl chloride (46 μL) were added under argon, and the mixture was stirred for one night at 55 °C. The usual workup afforded a residue that was purified by flash chromatography yielding [^{14}C]diuron (yield >95%, specific activity 60.3×10^6 Bq mmol^{-1}, radiochemical purity >97% as determined by radio-RP-HPLC analysis).

Plant Uptake. Seeds of wheat cv. Courtot and radish cv. Fluo were sown in quartz sand irrigated with either of a [^{14}C]diuron or a [^{14}C]linuron nutrient solution one-fourth strength Hoagland pH 6 (Sigma H-2395) (0.2 mg L^{-1}, 0.05 mg/kg substrate, 50 kBq). They were grown in a climate-controlled cabinet under a 16 h photoperiod at 22/19 °C (day/night) and 350 μmol m^{-2} s^{-1} photosynthetic photon-flux density (PPFD). Plants were irrigated at day 5 every other day with the Hoagland solution without herbicides. Treated plants were harvested after two weeks, quickly rinsed with acetone (a few seconds) to remove adsorbed residues on the surface, and frozen at −80 °C before further analysis.

Plant Metabolism. One-week-old plants were placed in glass tubes (95 × 13 mm) that contained either 1 mL of a [^{14}C]diuron or a [^{14}C]linuron nutrient solution (three plants, 25 μg and 8.33 kBq per tube). The uptake period, between 2 and 10 h, was followed by a water chase under a 120 h photoperiod (12, 24, 36, 48, 72, 96, and 120 h) for diuron and 120 h for linuron. Samples were then stored at −80 °C before extraction.

Extraction Procedures. Frozen plants were ground in a chilled mortar. An aliquot of the resulting powder was kept to measure the total radioactivity taken up by plants. Ground tissues were transferred in methanol/dichloromethane/water (2:1:0.8, v/v/v), homogenized for 4 h in a vortex (30 s every 15 min) and stored overnight at −20 °C. The resulting extract was then sonicated with an ultrasonic cell disrupter (Branson sonifier 450, Fisher Bioblock, Illkirch, France) for 5 min and centrifuged at 10000*g* for 10 min. The pellet was washed two times with the solvent mixture. The three supernatants, which contained the extractable residues, were combined and evaporated to 10 mL under vacuum. The extractable residues were then further purified by solid phase extraction on LC-18 cartridges (5 g, 20 mL, Supelclean ENVI-18 SPE tubes, Supelco, Saint Quentin Fallavier, France) and eluted with 80% methanol. Eluates, which contained all of the radioactivity were dried under vacuum up to 50 μL and stored at −80 °C until preparation for HPLC analysis. The pellets, consisting of the nonextractable residues, were allowed to air-dry for 24 h at room temperature to remove organic solvents, and then freeze-dried for 60 h to remove water.

Enzymatic and Chemical Hydrolysis Procedures. All the samples, which contained about 85 Bq, were evaporated to dryness under vacuum or a nitrogen stream before treatment by enzymes or hydrolysis.

β-D-Glucosidase Hydrolysis. Samples were incubated with one unit of almond β-glucosidase in 200 of μL 0.1 M pH 5.0 sodium acetate buffer at 30 °C for 2 h.

Esterase Hydrolysis. Samples were treated with two units of rabbit liver esterase in 200 μL of 0.05 M pH 7.5 potassium phosphate buffer at 30 °C for 10 min.

Acid Hydrolysis. Samples were dissolved in 200 μL of 2 N HCl and heated at 100 °C for 2 h.

Alkaline Hydrolysis. Samples were dissolved in 200 μL of 0.1 N NaOH at 50 °C for 1 h.

After acid hydrolysis, distilled water was added to the samples, while after alkaline hydrolysis, samples were acidified to pH 3 with 2 N HCl. Radioactivity was extracted from the aqueous phase using diethyl ether (1:1, v/v). The ether fraction was evaporated, and the dry residue was reconstituted in the appropriate HPLC mobile phase.

Application of [^{14}C]Linuron to Tobacco Cell Cultures and Preparation of Cell Extracts. Tobacco cell suspension cultures (*Nicotiana tabacum* BY2) were grown in the dark at 25 °C in 1 L Erlenmeyer flasks containing 250 mL of Murashige and Skoog medium (Sigma M-5524) supplemented with vitamins and plant growth regulators: KH_2PO_4 (200 mg L^{-1}), sucrose (30 g L^{-1}), myoinositol (100 mg L^{-1}), thiamine (10 mg L^{-1}), and 2,4-dichlorophenoxyacetic acid (1×10^{-6} mol L^{-1}). The medium was adjusted to pH 5.8. Cells (25 mL) were transferred every week into fresh sterile medium to maintain the culture in exponential growth. A 1,000 μg sample of unlabeled linuron and one of 3.33×10^5 Bq of [^{14}C]linuron (240 μL, dissolved in ethanol) were added to the culture medium five days after transfer into fresh medium. Incubation was ended 72 h after treatment. Cells were separated from the medium by centrifugation at 3000*g* for 10 min, and the pellet, corresponding to the cells, was washed twice with water. Cells were extracted, purified, and stored as described above. Medium was freeze-dried for 60 h to remove water, purified, and stored as described above.

Determination of Radioactivity. Radioactivity of plant parts and of nonextractable residues was measured after oxidative combustion of aliquots in an oxidizer (model Packard 307, PerkinElmer Life and Analytical Sciences, Courtaboeuf, France). The resulting $^{14}CO_2$ was trapped in a scintillation mixture (Permafluor and Carbosorb, PerkinElmer LAS) and counted in a Packard Tricarb 2200CA scintillation counter. Aliquots of extractable residues were directly counted with Ultimagold (PerkinElmer LAS) as scintillation cocktail. Amounts of residues were calculated from the specific activity of diuron and linuron, as equivalent parent compound.

Chromatography. Analyses by HPLC were performed on a Spectra-Physics P4000 (Les Ulis, France) liquid chromatograph equipped with a P1000 Spectra-Physics ultraviolet detector set at 245 nm. Radioactivity was monitored with an online Flo-One β A500 scintillation detector (cell volume, 0.5 mL; scintillation cocktail ratio, 2 mL scintillation liquid mL^{-1} HPLC effluent) (PerkinElmer LAS), operating with Flo-Scint II scintillation counting cocktail (PerkinElmer LAS). Separations of diuron or linuron and related metabolites were carried out on a 5.0 μm Prontosil (Bischoff Chromatography, Leonberg, Germany) reverse phase column (250 × 4.6 mm) with a guard cartridge. Elution was performed at 30 °C with a flow rate of 1 mL min^{-1}. For diuron the column was equilibrated with a mixture of 85.5% of solvent A (water/acetonitrile, 95:5, v/v) and 14.5% of solvent B (water/acetonitrile, 60:40, v/v). Elution conditions were as follows: a 15 min linear increase of solvent B from 14.5% to 85.5%, 85.5% solvent B for 15 min, a linear increase to 20% solvent B and 80% solvent C (acetonitrile 100%) and 20% solvent B/80% solvent C for 5 min. Retention times of diuron and its metabolites are given in **Table 1**. For linuron the column was equilibrated with 100% of solvent A. Elution conditions were as follows: a linear gradient of solvent B from 0 to 85.5% for 30 min, 85.5% of solvent B for 10 min (tobacco cells) or 15 min (wheat and radish), a linear increase to 20% solvent B and 80% solvent C and 20% solvent B/80% solvent C for 10 min. Retention times of linuron and metabolites are given in **Table 2**.

Isolation of Metabolites. Metabolites and the parent compound (extractable residues) were isolated by coupling the HPLC system with a fraction collector (model FC-204, Gilson Medical Electronics, Middleton, WI) set at 4 fractions min^{-1}. An aliquot of each fraction was counted in a scintillation counter to monitor radioactivity. The fractions of each peak were combined and evaporated to dryness under vacuum. Each peak was then purified by solid phase extraction on C18 cartridges (Supelco) and

Table 1. LC and MS Characteristics of Diuron Metabolites in Wheat and Radish

metabolite	peak no. (**Figure 1**)	t_R in HPLC (min)	*m/z* $[M-H]^-$ or $[M+H]^+$	*m/z* precursor ion	*m/z* main fragment ions[a]
3-(3,4-dichlorophenyl)-1-hydroxymethyl-*O*-glucose-1-methylurea	1	16.1	395/397/399	395	233, 203*
				397	235, 205*
3-(3,4-dichlorophenyl)-1-hydroxymethyl-*O*-glucose-urea	1	16.1	409/411/413	409	247, 217*
				411	249, 219*
3-(3,4-dichlorophenyl)-1-hydroxymethylurea	2	19.3	233/235/237	233	203, 160*
				235	205, 162*
3-(3,4-dichlorophenyl)urea	3	21.4	205/207/209	205	162, 188
				207	164, 190
3-(3,4-dichlorophenyl)-1-methylurea	4	24.0	219/221/223	221	162
				223	164

[a] The symbol * refers to fragment ions obtained by MS^3 experiments.

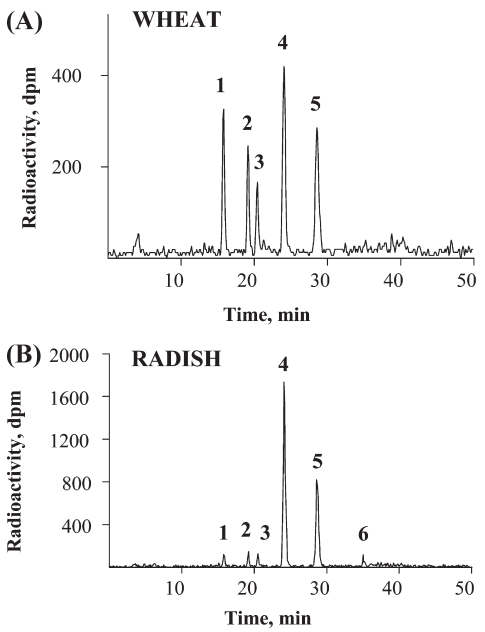

Figure 1. Typical radio-reverse-HPLC chromatograms of extractable residues obtained from crude extracts of (**A**) wheat and (**B**) radish treated with [^{14}C]diuron. Peak 5: diuron, peak 6: 3,4-dichloroanilin. Metabolite names and retention times of peaks 1, 2, 3, and 4 are given in **Table 1**.

eluted with increasing concentrations of methanol. Eluates from 40 to 60%, depending on each peak, that contained the maximum of radioactivity were dried under vacuum and stored at −20 °C until analysis by MS or ^{1}H NMR.

Mass Spectrometry. Structural characterization of the purified metabolites was conducted on a quadrupole ion trap mass spectrometer (Finnigan LCQ, Thermo Finnigan, Les Ulis, France) fitted with an electrospray ionization source. To obtain complementary information, both positive (PI-ESI) and negative ionization (NI-ESI) modes were used. Samples (typically 1 ng μL^{-1} in MeOH/H_2O (50:50, v/v)) were introduced into the ionization source at a flow rate of 5 μL min^{-1}. The heated transfer capillary was maintained at 220 °C. Operating parameters for production and transmission of electrosprayed ions into the ion trap analyzer (needle voltage, nebulizing gas flow rate, transfer capillary voltage, tube lens offset, etc.) were optimized for each compound to achieve maximum sensitivity. All other parameters for MS/MS experiments (isolation width, excitation voltage, excitation time) were also adjusted to obtain maximum structural information about the compound of interest. All analyses were performed under automatic gain control conditions using helium as damping as well as collision gas for MS/MS experiments. Tandem mass spectrometric experiments were performed on quasi molecular ions of the two most abundant isotopic peaks of compounds bearing two chloride atoms. The two atomic mass unit (amu) difference of the fragment ion *m/z* ratio was used for identifying chlorinated fragment ions, and therefore the dichlorophenyl ring (**Tables 1** and **2**).

Nuclear Magnetic Resonance Spectroscopy. NMR spectra were obtained at 300 K using a Bruker Avance DRX-600 spectrometer (Bruker, Wissembourg, France), operating at 600.13 MHz and equipped with a 5 mm H,C,N inverse triple resonance TXI cryoprobe attached to a cryoplatform (the preamplifier unit). Samples were dissolved in 600 μL of deuterated methanol (CD_3OD).

One-dimensional ^{1}H NMR spectra (**Table 3**) were acquired using a standard pulse sequence for ^{1}H NMR. 1024 free induction decays (FIDs) were collected with a spectral width of 12 ppm in 64 K data points. An exponential function equivalent to a line-broadening of 0.3 Hz was applied prior to Fourier transformation.

Two dimensional ^{1}H−^{1}H COSY (correlation spectroscopy) NMR spectra were acquired over a spectral width of 12 ppm in both dimensions, in 1024 data points in the F1 dimension and 512 data points in the F2 dimension. Sixty-four FIDs were collected per data point in the F2 dimension. A sine-bell apodization function was applied to both F1 and F2 dimensions before Fourier transformation.

Data Analysis. Results, expressed as micrograms of equivalent parent compound per gram, were always relative to DW. They were the average of at least three to six measurements for each experiment and were analyzed for statistical significance by two-tailed Student's *t* test ($p < 0.05$).

RESULTS AND DISCUSSION

Uptake and Distribution of [^{14}C]Diuron and [^{14}C]Linuron in Wheat and Radish. The results of the uptake of [^{14}C]diuron and [^{14}C]linuron in wheat and radish whole plants are shown in **Table 4**. The amount of radioactivity absorbed by plants and left in the nutrient solution accounted for the total applied radioactivity. Wheat and radish plants have taken up [^{14}C]diuron and [^{14}C]linuron. The octanol−water partition coefficient, particularly log K_{ow}, is often used as a key parameter in the estimation of plant absorption of xenobiotics and translocation within plants following root uptake. Uptake of organic chemicals is reported to be efficient for compounds with log K_{ow} values comprised between 1 and 3.5 (*24*). This result was thus expected as log K_{ow} values of diuron and linuron are 2.68 and 3, respectively (*8*, *25*). Due to their negative pK_a values (no dissociation) (*26*), diuron and linuron are expected to be neutral around pH values of plant compartments (pH 5, xylem and vacuoles or pH 7, cytoplasm and phloem), and consequently to enter roots in almost equal quantities. Uptake of both compounds was equivalent in a same plant but appeared to be higher for radish than that in wheat plants (**Table 4**). Apparent differences in the uptake of [^{14}C]herbicides between a monocotyledonous (oat, wheat) and dicotyledonous (soybean) plant have already been reported (*27*, *28*).

Diuron and linuron are efficiently translocated into aerial plant parts since nearly 60% of the total amount of residues was associated with aerial parts in wheat and 72% in the case of radish. The

Table 2. LC and MS Characteristics of Linuron Metabolites in Tobacco Cells, Radish and Wheat

metabolite[a]	t_R (min) HPLC (peak no.)	$[M - H]^-$ (*m*/*z*)	*m*/*z*	
			precursor ion	main fragment ions
3-(3,4-dichlorophenyl)-1-*O*-glucose-1-methylurea	32.2 (T1)	395/397/399	395	233, 160, 217, 208
			397	235, 162, 219, 208
3-(3,4-dichlorophenyl)-1-methoxyurea	40.2 (T2, R4, W5)	233/235/237	233	160, 201, 173
			235	162, 203, 175
R-1-glucose-1-methoxyurea	28.0 (R1)	395/397/399	395	208, 243, 176
			397	208, 245, 176
nonidentified	35.0 (R2)	531/533/535	531	327, 369
			533	327, 369
nonidentified	39.0 (R3)	401/403/405	401	183, 357, 383
			403	183, 359, 385
R-1-acetylglucose-1-methoxyurea or R-1-*O*-acetylglucose-1-methylurea	18.5 (W1a)	437/439/441	437	250, 190, 377
			439	250, 190, 379
R-1-hydroxymethyl-acetylglucose-1-methoxyurea or R-1-*O*-hydroxymethyl-acetylglucose-1-methylurea	18.5 (W1b)	467/469/471	467	221, 408, 161
			469	221, 410, 161
R-1-hydroxymethyl-glucose-1-methoxyurea or R-1-*O*-hydroxymethyl-glucose-1-methylurea	28.5 (W2)	425/427/429	425	179, 335, 161, 263, 366, 143
			427	179, 337, 161, 265, 368, 143
R-1-hydroxymethyl-1-methoxyurea or R-1-*O*-hydroxymethyl-1-methylurea	34.3 (W3)	263/265/267	263	203
			265	205
R-1-hydroxy-1-methylurea	38.7 (W4)	233/235/237	233	160, 201, 173
			235	162, 203, 175

[a] R = 3-(3,4-dichlorophenyl).

Table 3. Summary of ^{1}H NMR Resonances of Isolated Metabolites[a]

compound	aglycon moiety	glycoside
3-(3,4-dichlorophenyl)-1-*O*-glucose-1-methylurea (T1)	H-2: 7.72 (d, 2.0)	H-1′: 5.70 (d, 8.5)
	H-5: 7.35 (d, 8.5)	H-2′: 3.85 (m)
	H-6: 7.21 (dd, 8.5 and 2.0)	H-3′: 3.65 (m)
	N−CH_3: 3.21 (*s*)	H-4′: 3.79 (m)
		H-5′: 3.54 (m)
		H-6′: 4.05 (dd, 6.6 and 11.6); 4.14 (dd, 4.4 and 11.6)
3-(3,4-dichlorophenyl)-1-methoxyurea (T2-W5)	H-2: 7.82 (d, 2.0)	
	H-5: 7.40 (d, 8.5)	
	H-6: 7.44 (dd, 8.5 and 2.0)	
	O−CH_3: 3.71 (s)	
linuron	H-2: 7.82 (d, 2.0)	
	H-5: 7.40 (d, 8.5)	
	H-6: 7.45 (dd, 8.5 and 2.0)	
	N−CH_3: 3.15 (s)	
	O−CH_3: 3.75 (s)	

[a] Chemical shifts (ppm) are relative to deuterated methanol (1H, δ, 3.30). Multiplicity of signals: s = singlet, d = doublet, dd = doublet of doublets, ddd = doublet of doublet of doublets, t = triplet, and m = multiplet. Values in parentheses are ^{1}H−^{1}H splittings (Hz) in cases where these are clearly resolved.

Table 4. Uptake of [^{14}C]Diuron and Uptake, Extractable Residues (ER), and Nonextractable Residues (NER) of [^{14}C]Linuron in Wheat and Radish[a]

	wheat			radish		
	plant	aerial parts	roots	plant	aerial parts	roots
[^{14}C]diuron	1.62 ± 0.31	1.83 ± 0.22	1.54 ± 0.20	2.91 ± 0.32	3.65 ± 0.32	1.33 ± 0.21
	(17.5 ± 2.4)	(11.6 ± 1.9)	(5.9 ± 1.1)	(24.0 ± 3.6)	(15.6 ± 2.9)	(8.4 ± 1.2)
[^{14}C]linuron	1.75 ± 0.15	1.65 ± 0.25	1.93 ± 0.13	3.26 ± 0.44	4.37 ± 0.35	2.06 ± 0.29
	(18.5 ± 2.3)	(10.9 ± 1.7)	(7.6 ± 0.7)	(26.6 ± 4.1)	(19.1 ± 3.7)	(7.5 ± 0.8)
[^{14}C]-ER	0.87[b] ± 0.08	1.07[b] ± 0.15	0.55[b] ± 0.04	2.15[b] ± 0.25	3.02[b] ± 0.20	1.14[b] ± 0.1
	(9.2 ± 1.3)	(7.0 ± 0.9)	(2.2 ± 0.4)	(17.5 ± 2.3)	(13.2 ± 2.3)	(4.3 ± 0.6)
[^{14}C]-NER	0.52[b] ± 0.12	0.20[b] ± 0.04	1.05[b] ± 0.20	0.40[b] ± 0.03	0.25[b] ± 0.05	0.57[b] ± 0.04
	(5.5 ± 1.3)	(1.3 ± 0.3)	(4.2 ± 1.1)	(3.26 ± 0.4)	(1.1 ± 0.3)	(2.2 ± 0.3)

[a] Results are expressed as micrograms of equivalent parent compound per gram DW or as percentage of the applied radioactivity (parentheses). Values are means ± SD from at least three samples. [b] Statistically significant, ER compared to NER ($p < 0.05$).

partition of the herbicides between roots and aerial parts is in agreement with their use as soil-applied, root-absorbed systemic herbicides. Autoradiography of a longitudinal section of radish treated with [^{14}C]linuron illustrated the accumulation of radioactivity in stems and leaves (not shown). This result was also in accordance with the log K_{ow} values of diuron and linuron, which are optimal not only for uptake but also for translocation. Due to their physicochemical characteristics, diuron and linuron are mainly carried by the transpiration stream via the xylem pathway. The larger development of radish leaves, compared to wheat,

could increase the transpiration stream and thus the translocation of the herbicides from roots to aerial parts. In addition, after penetration of xenobiotics, plants are able to metabolize these compounds. Metabolism generally modifies polarity of residues and consequently the distribution in plants. Differences in translocation between plant species were already noticed by Walker and Featherstone (*29*), who have also suggested that tolerance of seedlings to linuron resulted from root fixation and shoot metabolism. In our study, it is worth noting that wheat plants were more tolerant to diuron and linuron than radish plants. Phytotoxic symptoms (bleaching, necrotic spots) appeared in leaf extremities of radish at concentrations as low as 1−2 mg L^{-1} (0.25−0.5 mg/kg sand) of diuron or linuron while wheat plants were apparently not affected at concentrations up to 10 mg L^{-1} (2.5 mg/kg sand).

Analysis of the distribution of [^{14}C]diuron was not performed. The partitioning of the extractable and nonextractable residues of [^{14}C]linuron in wheat and radish is shown in **Table 4**. Most of the radioactivity was located in the extractable fraction at the expense of the nonextractable residues, particularly in radish plants. It should be noted that, owing to small quantities and to the relative heterogeneity of aliquots, variability in the 10−20% range was observed between total uptake and the sum of extractable + nonextractable residues. Extractable residues amounted to 17.5% of the total applied radioactivity in radish plants and 9.2% in wheat plants whereas nonextractable residues represented only 5.5% and 3.3% in wheat and radish plants, respectively. Nearly 85% of the total residues were located in the extractable fraction in radish, and nonextractable residues represented 37% of total residues in wheat. These results were in agreement with the differences observed in the distribution of radioactivity between soluble and bound residues in wheat and radish since radish plants translocated very efficiently residues to aerial parts, which contained more extractable residues than nonextractable residues. Differences in cell wall structures could partly explain lower amounts of nonextractable residues in dicotyledonous compared with monocotyledonous plants (*30*) but could also be due to differences in degradation rate between the two plants. In leaves, the majority of radioactivity was found to be associated with the extractable residues, 84% and 92% for wheat and radish, respectively. Nonextractable residues were mainly recovered in roots, especially in wheat where their amount was 2-fold higher than those of extractable residues. The higher proportion of nonextractable residues associated with roots compared to aerial parts was already reported for chloroanilines and chlorophenols (*31*, *32*). The relative tolerance of wheat could be explained by the higher amount of nonextractable residues as they are generally less toxic for plants (*33*). In addition, metabolism of herbicides and sequestration of residues in roots lower their translocation to aerial parts.

Identification of Extractable Residues of [^{14}C]Diuron in Wheat and Radish. *Identification of Metabolites*. Typical radio-HPLC chromatograms obtained from crude extracts of wheat showed the presence of four peaks in addition to diuron (peak 5, t_R = 29.5 min) (**Figure 1A**). From crude extracts of radish, five peaks appeared on the radio-HPLC profile (**Figure 1B**). Under our conditions, metabolization was not complete since the parent compound accounted for 26% in wheat and 34% in radish. In wheat, peak 4 (t_R = 24 min) was the most abundant, 44% of the total extractable metabolites (TER), but the three other peaks accounted for relatively high amounts, 24%, 19%, and 13% for peak 1 (t_R = 16 min), peak 2 (t_R = 19 min), and peak 3 (t_R = 21 min), respectively. In radish, most of the TER were metabolized to peak 4 (80%) and a sixth peak (t_R = 35.5 min) that eluted after the peak corresponding to diuron was detected. This peak was tentatively assigned to 3,4-dichloroaniline by coelution in HPLC with an authentic standard. Structures of the other metabolites were identified by comparison with retention times in HPLC of authentic standards, by enzymatic or chemical hydrolyses, and by MS analyses. Peak 3 and peak 4 coeluted in HPLC with 3-(3,4-dichlorophenyl)urea and 3-(3,4-dichlorophenyl)-1-methylurea, respectively. The structures of the two metabolites were further characterized using ESI-MS. Under positive ionization conditions, metabolite 3 yielded an isotopic cluster at *m*/*z* 205/207/209 characteristic of a dichlorinated compound. The observed *m*/*z* ratios of the MH^+ ions were in accordance with those of protonated (3,4-dichlorophenyl)urea. Decomposition of the *m*/*z* 205 and *m*/*z* 207 precursor ions upon MS/MS experiments gave rise to the *m*/*z* 162 and *m*/*z* 164 fragment ions, respectively, which could be attributed to dichloroaniline. Less abundant fragmentations were present at *m*/*z* 188 and 190, formed by loss of neutral NH_3 from the *m*/*z* 205 and 207 precursor ions, respectively. Based on these data, the chemical structure of metabolite 3 was therefore attributed to 3-(3,4-dichlorophenyl)urea (**Table 1**).

The positive ESI mass spectrum of metabolite 4 exhibited an MH^+ ion also displaying the characteristic isotopic pattern of a dichlorinated molecule at *m*/*z* 219/221/223. MS/MS spectra recorded from the *m*/*z* 219 and *m*/*z* 221 precursor ions also gave the *m*/*z* 162 and *m*/*z* 164 product ions, respectively, corresponding to protonated dichloroaniline. Metabolite 4 was thus identified as 3-(3,4-dichlorophenyl)-1-methylurea (**Table 1**).

Peak 1 was hydrolyzed by almond β-D-glucosidase to a product coeluting with peak 2, peak 4, and low amount of diuron and peak 3, suggesting the presence of metabolites conjugated to glucose in peak 1 and precursors in the other peaks. Hydrolysis by HCl provided peaks that corresponded to 3-(3,4-dichlorophenyl)urea (peak 3) and 3-(3,4-dichlorophenyl)-1-methylurea (peak 4). The peak was further submitted to MS analysis, which revealed the presence of two metabolites displaying $[M - H]^-$ ions at *m*/*z* 395/397/399 and 409/411/413 respectively, when analyzed in the negative ionization mode. Both isotopic clusters corresponded to dichlorinated species. Resonant excitation MS/MS experiments carried out on the *m*/*z* 395 and *m*/*z* 397 ions yielded characteristic fragment ions at *m*/*z* 233 and *m*/*z* 235 respectively, which could be attributed to the loss of a glucose moiety, further supported by the occurrence of the *m*/*z* 161 complementary ion together with the *m*/*z* 179 ion on both MS/MS spectra. Other fragment ions observed at *m*/*z* ratios greater than 233/235 (i.e., *m*/*z* 377/379, *m*/*z* 335/337, *m*/*z* 305/307) formed by cleavage of the hexosidic ring were also present. Consecutive decomposition of the *m*/*z* 233 and 235 ions in MS^3 experiments carried out in the ion trap gave the *m*/*z* 203 and 205 ions respectively, corresponding to the deprotonated form of dichlorophenyl-urea, arising from the elimination of a CH_2O group. This could be considered as diagnostic of the occurrence of an hydroxymethyl group on the molecule. These data were consistent with the fragmentation of 3-(3,4-dichlorophenyl)-1-hydroxymethyl-*O*-glucose-1-methylurea (**Table 1**). The MS/MS analysis of the precursor ions from the second isotopic cluster (*m*/*z* 409/411/413) showed that the *m*/*z* 409 ion mainly decomposed via the loss of a glucose moiety leading to the *m*/*z* 247 fragment ion. Other fragment ions formed from the cleavage of the glucose moiety were also observed (*m*/*z* 349/319/289). The MS^3 experiment carried out on the *m*/*z* 247 product ion led to a unique fragment ion at *m*/*z* 217, resulting from the loss of CH_2O and showing the occurrence of a hydroxymethyl group on the starting molecule. Similarly, the *m*/*z* 411 precursor ion led to the *m*/*z* 249 and *m*/*z* 219 ions as main product ions in MS^2 and MS^3 experiments, respectively. The structure of this metabolite was attributed to the glucoside of 3-(3,4-dichlorophenyl)-1-hydroxymethylurea (**Table 1**). The presence of two metabolites explained

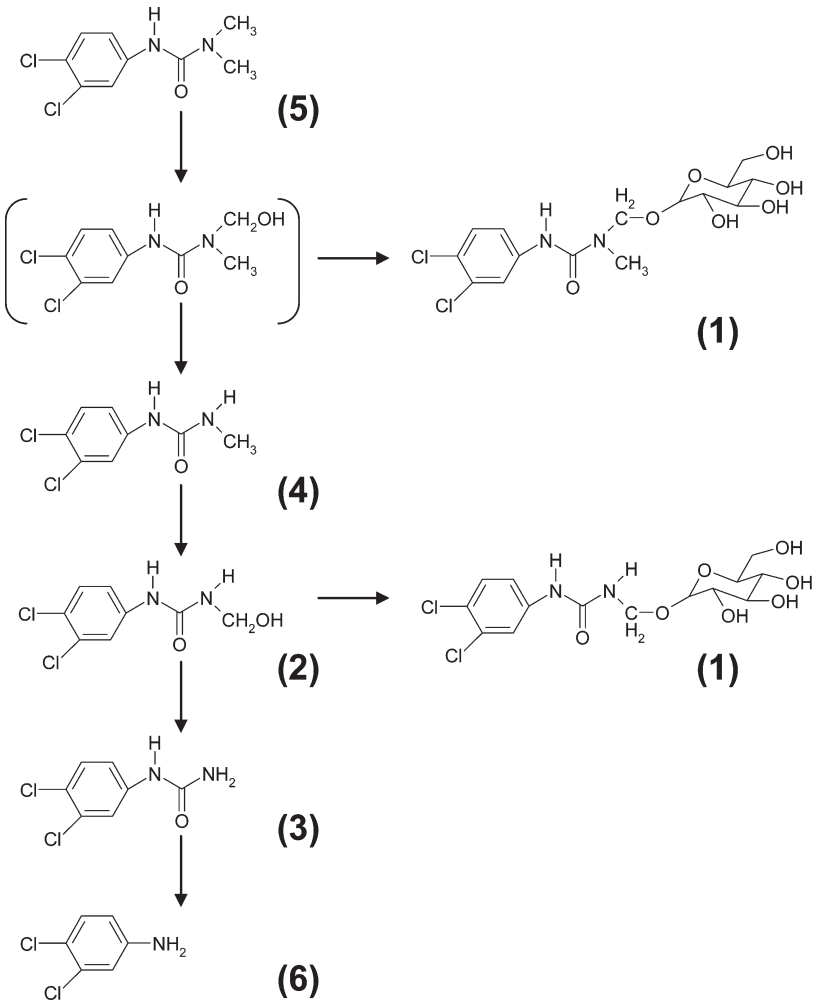

Figure 2. Proposed metabolic pathways of diuron in wheat and radish. HPLC peaks are given in parentheses.

the complex data obtained from enzymatic and chemical hydrolyses: the glucoside of 3-(3,4-dichlorophenyl)-1-hydroxymethyl-urea leading to peaks 2 and 3 and the glucoside of 3-(3,4-dichlorophenyl)-1-hydroxymethyl-1-methylurea to peak 4, and diuron.

The isotopic cluster observed at *m*/*z* 233/235/237 on the NI/ESI mass spectrum of metabolite 2 clearly indicated the presence of the dichloroaniline moiety in this metabolite. The MS/MS spectrum recorded from the *m*/*z* 233 ion showed the loss of CH_2O yielding the *m*/*z* 203 fragment ion, which eliminated NH═C═O to give the *m*/*z* 160 ion in a subsequent MS^3 experiment. These data were further supported by similar results obtained from the *m*/*z* 235 precursor ion, allowing 3-(3,4-dichlorophenyl)-1-hydroxymethylurea to be proposed as the possible structure for metabolite 2 (**Table 1**).

Characterization of these metabolites showed that the degradation of diuron led to 3-(3,4-dichlorophenyl)urea and thereafter 3,4-dichloroaniline as final metabolites (**Figure 2**) following successive loss of two methyl groups, as already described by Frear et al. (*16*). N-Demethylation reactions generally proceed by initial hydroxylation of methyl groups by cytochrome P-450 monooxygenases (*34*). However, we did not succeed in isolating the first hydroxylated derivate of diuron (**Figure 2**, in brackets), probably due to its short lifetime and its weak stability during extraction. We previously noticed that hydrolysis of the glucoside conjugate of this compound did not allow its detection in HPLC, on the contrary to the monomethyl hydroxylated derivate (metabolite 2). Furthermore, the first reaction of oxidation could be a rate-limiting step and the resulting product would be rapidly metabolized. This compound was also not detected in the metabolism of [^{14}C]diuron in spinach leaves (*17*). The hydroxylated compounds led to the formation of two metabolites conjugated to glucose that block the demethylation process and generated two new final metabolites. Conjugation to glucose is the most frequent pesticide detoxification pathway in plants (*35*), which possess a large variety of glycosyltransferases able to conjugate both endogenous compounds and xenobiotics (*19*, *36*). Metabolism of diuron is more efficient in wheat than in radish, and this could be connected to the higher tolerance of wheat to this herbicide. In radish, degradation to monodesmethyl-diuron induces only a partial detoxification since monodealkylated herbicides like monuron and chlorotoluron still exhibit a biological activity whereas N-dealkylated herbicides lead to inactive compounds (*37*).

Kinetics of Formation of [^{14}*C*]*Diuron Metabolites*. At 12 and 24 h, only two peaks that corresponded to diuron and 3-(3,4-dichlorophenyl)-1-methylurea were detected on radiochromatograms. After 36 h of metabolization, glucoside conjugates and 3-(3,4-dichlorophenyl)-1-hydroxymethyl-urea appeared. Finally, 3-(3,4-dichlorophenyl)urea was found after 48 h. The second hydroxylation reaction could also be a rate-limiting step since the substrate accumulated in comparison to other metabolites. These data were in accordance with the metabolic pathway proposed in **Figure 2**.

Identification of Extractable Residues of [^{14}C]Linuron in Tobacco Cells, Wheat, and Radish. Typical radio-HPLC profiles obtained after treatment with [^{14}C]linuron in tobacco cells, wheat, and radish are shown in **Figure 3**. In tobacco cells, the rate of

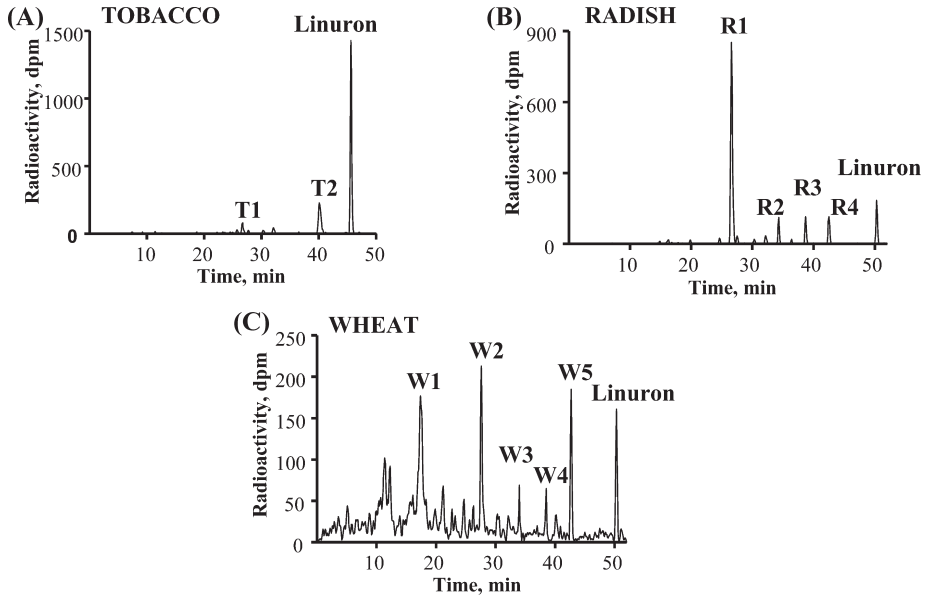

Figure 3. Typical radio-reverse-HPLC chromatograms of extractable residues obtained from crude extracts of (**A**) tobacco cells, (**B**) radish, and (**C**) wheat treated with [^{14}C]linuron. Elution conditions were shortened of 5 min for tobacco cells. Metabolite names and retention times are given in **Table 2**.

metabolization was weak (30%) and enabled apparition of early metabolites. This low metabolism was probably due to phytotoxicity. In addition to the peak of linuron (t_R = 45.7 min), the profile showed one peak at t_R = 40.2 min (metabolite T2) in relatively high amount (20%) and a minor peak at 27 min (metabolite T1) accounting for less than 5% of the radioactivity (**Figure 3A**). Under negative electrospray ionization conditions, the $[M - H]^-$ ion of metabolite T2 was observed at m/z 233 and displayed the characteristic isotopic pattern of a dichlorinated molecule. This could correspond to a demethylated form of linuron. The MS/MS spectrum generated from the m/z 233 ion exhibited two fragment ions at m/z 160 and 201, respectively. The same experiment carried out on the m/z 235 ion (^{37}Cl isotopic peak) selected as the precursor ion led to the m/z 162 and 203 fragment ions, respectively, indicating that both fragment ions contained the chlorine atoms. The m/z 160 fragment ion could thus be attributed to the deprotonated form of 3,4-dichloroaniline. Alternatively, the elimination of CH_3OH from the m/z 233 precursor ion explained the formation of the m/z 201 ion, suggesting that the methoxy function was still present on the $[M - H]^-$ ion. This metabolite was thus identified as 3-(3,4-dichlorophenyl)-1-methoxyurea (**Table 2**).

The negative ESI-MS analysis of metabolite T1 yielded a $[M - H]^-$ ion at m/z 395 consistent with a glucoside conjugate of monodemethylated linuron. The corresponding MS/MS spectrum displayed characteristic fragment ions at m/z 160, 208, 217 and 233, respectively. The same experiment was conducted on the m/z 397 precursor ion (^{37}Cl isotopic peak) and yielded the m/z 162, 208, 219, and 235 product ions, respectively, indicating that only the m/z 208 fragment ion did not contain the chlorine atoms. The occurrence of both the m/z 217 (219) and m/z 233 (235) ions on the MS/MS spectra was indicative of the presence of an O-glucoside rather than an N-glucoside, as presented in **Figure 4A**. From these data, 3-(3,4-dichlorophenyl)-1-*O*-glucose-1-methylurea could be proposed as a structure for metabolite T1 (**Table 2**).

These metabolites were also analyzed by ^{1}H NMR spectroscopy in order to establish whether the methyl or the methoxy group was removed under our conditions and to locate precisely the glucose molecule. The ^{1}H chemical shifts of these two metabolites are summarized in **Table 3**. By comparison with the ^{1}H NMR spectrum of linuron, the presence of the methoxy group at 3.71 ppm in the ^{1}H NMR spectrum of metabolite T2 and the disappearance of the methyl linked to the nitrogen at 3.15 ppm indicated that the methoxy group was still present in the molecule. The metabolite T2 was unambiguously identified as 3-(3,4-dichlorophenyl)-1-methoxyurea (**Table 3**).

The ^{1}H NMR spectrum of metabolite T1 showed a doublet at 7.72 ppm, a doublet at 7.35 ppm and a doublet of doublets at 7.21 ppm in the aromatic region corresponding to the protons of aglycon moiety. In the aliphatic region, the signals at 5.70, 3.85, 3.65, 3.79, 3.54, 4.05, and 4.14 ppm indicated the presence of a glycoside conjugated to linuron. The signal corresponding to the anomeric proton was a doublet, and the high coupling constant (8.50 Hz) indicated that this glycoside was probably β-glucose. The signal at 3.21 ppm corresponding to the methyl group indicated that the methyl group was probably linked to the nitrogen. These observations were in agreement with the MS data and confirmed that metabolite T1 was probably 3-(3,4-dichlorophenyl)-1-*O*-glucose-1-methylurea (**Table 3**).

In radish, the rate of metabolization was 84%. Linuron (t_R = 50.4 min) was converted into one main metabolite (R1, t_R = 28.0 min) that accounted for 78% of the TER (**Figure 3B**). This peak was further analyzed by negative ESI-MS and yielded a $[M - H]^-$ ion at m/z 395, consistent with a glucoside conjugate of monodemethylated linuron. However, the MS/MS spectrum of this peak, presented in **Figure 4B**, was not identical to that of metabolite T1 in tobacco (**Figure 4A**), and displayed m/z 208 as the base peak (**Table 2**). The m/z ratio of this fragment ion was not shifted at m/z 210 when performing an MS/MS experiment on the m/z 397 (^{37}Cl isotopic peak) precursor ion. Based on these data, this peak was tentatively identified as 3-(3,4-dichlorophenyl)-1-glucosyl-1-methoxyurea. The high intensity of the m/z 208 ion and some weak abundance ions detected at m/z 243 (shifted at m/z 245) could be explained by the relative strength of the N-glycosidic bond compared to an O-glycosidic one.

Beside this major peak, three other minor metabolites were detected on the chromatogram presented in **Figure 3B**, and exhibited retention times of 35 min (R2, 7% TER), 39 min (R3, 7% TER) and 42 min (R4, 7% TER), respectively. The mass spectrometric analysis of R2 and R3 yielded $[M - H]^-$ ions at m/z 531 and m/z 401 respectively, both displaying the characteristic isotopic pattern of a dichlorinated molecule. However, no characteristic

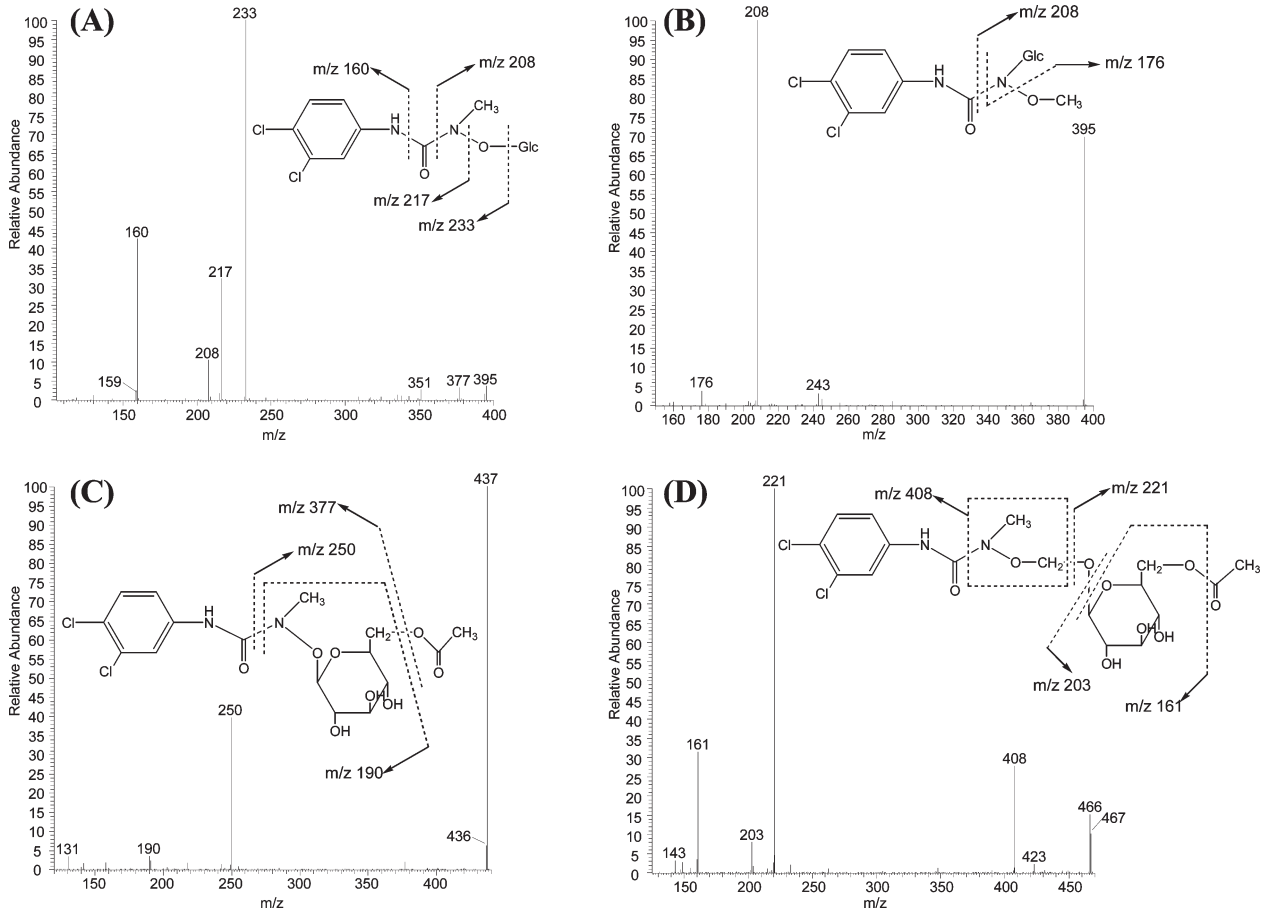

Figure 4. Product ion MS/MS spectra obtained from (**A**) *m/z* 395 precursor ion of metabolite T1, (**B**) *m/z* 395 precursor ion of metabolite R1, (**C**) *m/z* 437 precursor ion of metabolite W1a and (**D**) *m/z* 467 precursor ion of metabolite W1b.

information could be obtained from the corresponding MS/MS spectra of these metabolites. Although its retention time was slightly different, metabolite R4 (t_R = 42 min) was identified as 3-(3,4-dichlorophenyl)-1-methoxyurea (**Table 2**) as described above for metabolite T2 from tobacco cells.

In wheat, the rate of metabolization was 89% and a more complex pattern was obtained in HPLC (**Figure 3C**). Due to their low amounts and high polarities, only few peaks, numbered W1 to W5 in **Figure 3C**, could be successfully submitted to MS analysis. The negative ESI-MS spectrum of peak W1 (t_R = 18.5 min, 29.2% TER) displayed two isotopic clusters corresponding to dichlorinated molecules, respectively at *m/z* 437/439/441 and *m/z* 467/469/471, indicating that this peak contained two metabolites (W1a and W1b). MS/MS experiments carried out on the *m/z* 437 and 439 precursor ions both yielded the same major product ion at *m/z* 250 (**Figure 4C** and **Table 2**). This was consistent with the fragmentation of an acetylglucoside of monodemethylated linuron, considering the cleavage of the C−N bond of the urea moiety of metabolite W1a with charge retention on the non-chlorinated part of the molecule. However, the demethylation site could not be identified with these data. The MS/MS analysis of the *m/z* 467 and 469 ions from metabolite W1b yielded the *m/z* 221 ion, which was also observed as the same base peak on both spectra, together with several minor fragment ions listed in **Table 2**. The occurrence of the *m/z* 408 ion is noteworthy and cannot be explained without considering a complex rearrangement involving the elimination of $CH_2{=}N{-}O{-}CH_3$ from the urea moiety of the metabolite as represented in **Figure 4D**. This allowed an acetylglycoside conjugate of hydroxylated linuron to be proposed as a possible structure for W1b. Here again, it was not possible to determine whether the hydroxylation of linuron occurred on the 1-methyl or the 1-methoxy group of urea.

When analyzed by negative ESI-MS, peak W2 (t_R = 29 min, 18.1% TER) displayed a $[M-H]^-$ ion at *m/z* 425/427/429 consistent with a glucoside conjugate of hydroxylated linuron. This was confirmed by MS/MS experiments conducted on both *m/z* 425 and 427 ions, showing fragment ions at *m/z* 263 and 265, respectively, which could be considered as characteristic of the elimination of a glucose moiety from the $[M-H]^-$ precursor ions (**Table 2**). Note also the occurrence of the *m/z* 366 ion (shifted at *m/z* 368), which may also originate in the elimination of $CH_2{=}N{-}O{-}CH_3$ as mentioned above. The other product ions (*m/z* 179, 161, 143) were not shifted and could be attributed to the fragmentation of the glycosidic moiety of the conjugate.

The analysis of peak W3 (t_R = 34 min, 7.8% TER) yielded a $[M-H]^-$ ion at *m/z* 263 (^{35}Cl isotopic peak), which gave the *m/z* 203 fragment ion by resonant excitation MS/MS. This latter could be attributed to a deprotonated form of 3-(3,4-dichlorophenyl)urea, which was confirmed by the occurrence of the *m/z* 205 ion on the MS/MS spectrum of the *m/z* 265 precursor ion. This allowed to identify W3 as hydroxylated linuron, although the hydroxylation position could not be located.

Peaks W4 and W5 both gave the same spectra as peaks R4 (radish) and T2 (tobacco cells). The NMR analysis of W5 (t_R = 42.7 min, 14.1% TER) allowed this metabolite to be identified as 3-(3,4-dichlorophenyl)-1-methoxyurea (**Table 3**). Due to its low abundance, peak W4 (t_R = 38.5 min, 6.7% TER) could not be analyzed by NMR analysis. This metabolite was thus tentatively identified as 3-(3,4-dichlorophenyl)-1-hydroxy-1-methylurea (**Table 2**).

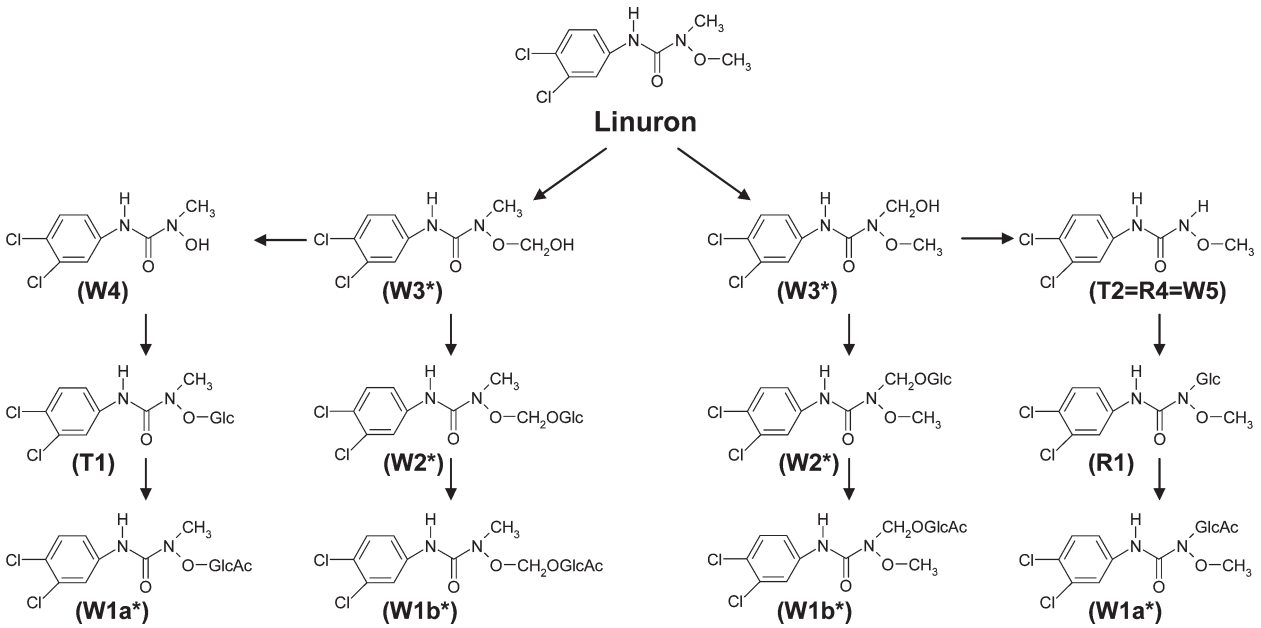

Figure 5. Proposed metabolic pathways of linuron in wheat and radish. HPLC peaks are given in parentheses. *For compounds W1a, W1b, W2, and W3, the hydroxylation position could not be located.

Both plant species share a common metabolism for linuron and diuron as demethylation and/or demethoxylation were characterized as final metabolites. It is noteworthy that we essentially found monodemethylated products of linuron (**Figure 5**), even in wheat where demethylated products of diuron were identified. However, several glucose conjugates of monomethyl- and desmethyl-diuron or linuron were evidenced for the first time in these plants. It is conceivable that demethylation reactions were step-limiting and that their substrates, still exhibiting phytotoxicity, were rapidly transformed by glycosyltransferases, which are abundant in plants especially in wheat (*38*). Glucoside conjugates were also described in spinach by Suzuki and Casida (*17*) during the metabolism of methazole (2-(3,4-dichlorophenyl)-4-methyl-1,2,4-oxadiazolidine-3,5-dione), an herbicide of the oxadiazolone class. However, glucose was conjugated to the nitrogen atom (N3) directly linked to the benzene ring, subsequently to opening of the azolidine ring. Such a metabolite was expected following treatment with [^{14}C]diuron but was not evidenced by the authors. On the contrary, 3-(3,4-dichlorophenyl)-3-hydroxy-1-methylurea was identified by HPLC−mass spectrometry from microsomal fractions of mouse incubated with [^{14}C]diuron (*17*) and 3-(6-hydroxy-3,4-dichlorophenyl)urea from microsomal fractions of rabbit incubated with linuron (*15*). Following oral ingestion, animals or humans can be exposed to glucoside conjugates. An important point in plant metabolism of xenobiotics is the possible bioavailability of the glycoside conjugates and the parallel that can be established with natural glycosides, in particular the bioavailability of natural phenolics with regard to their glycosylation pattern. Flavonoids mainly occur as glycosides in food. Glucosides of quercetin, a major dietary flavonoid, were more efficiently absorbed than quercetin itself. Moreover, the nature and the number of sugar units will determine the extent of small intestinal absorption of quercetin (*23*, *39*). Hollman et al. (*21*) have already mentioned the predominant role of the glycosyl part in the bioavailability of dietary quercetin in humans. These compounds could be then hydrolyzed by enzymes and microorganisms present in the digestive tract and be further metabolized into possibly toxic compounds. It is necessary to examine more carefully glycosyl conjugates of xenobiotics and particularly to evaluate their bioavailability in food chains. A better absorption and consequently a greater bioavailability of this kind of phase II metabolites could increase the toxicological risk of chemicals.

In conclusion, uptake of [^{14}C]diuron and [^{14}C]linuron was nearly equivalent in wheat and radish but translocation of parent compounds and related metabolites from roots to aerial parts was higher in radish. Characterization of extractable residues showed that the degradation of diuron and linuron should result in the formation of 3-(3,4-dichlorophenyl)urea following successive loss of methyl and/or methoxy groups. These oxidative N-demethylation and N-demethoxylation reactions also led to new glucoside conjugates. Glucose conjugation is a frequent inactivation reaction in plants. However, glycosylated compounds could be better absorbed and more bioavailable to food chains than their aglycon counterparts. They could be further hydrolyzed in the digestive tract of animals and metabolized to possibly toxic molecules. In addition, 3-(3,4-dichlorophenyl)urea represents a potential risk in food chains since this metabolite leads to the formation of 3,4-dichloroaniline, which is potentially toxic for animals.

ABBREVIATIONS USED

amu, atomic mass unit; DW, dry weight; ER, extractable residues; ESI-MS, electrospray ionization-mass spectrometry; K_{ow}, octanol−water partition coefficient; NER, nonextractable residues; NMR, nuclear magnetic resonance; RP-HPLC, reverse-phase high performance liquid chromatography; t_R, retention time; TER, total extractable residues.

LITERATURE CITED

(1) Tixier, C.; Sancelme, M.; Aït-Aïssa, S.; Widehem, P.; Bonnemoy, F.; Cuer, A.; Truffaut, N.; Veschambre, H. Biotransformation of phenylurea herbicides by a soil bacterial strain, *Arthrobacter* sp. N2: structure, ecotoxicity and fate of diuron metabolite with soil fungi. *Chemosphere* **2002**, *46*, 519−526.

(2) Ducruet, J. M. Les inhibiteurs du photosystème II. In *Les herbicides: Mode d'Action et Principes d'Utilisation*; Scalla, R., Ed.; INRA: Paris, France, 1991; pp 79−114.

(3) Cullington, J. E.; Walker, A. Rapid biodegradation of diuron and other phenylurea herbicides by a soil bacterium. *Soil Biol. Biochem.* **1999**, *31*, 677−686.

(4) Giacomazzi, S.; Cochet, N. Environmental impact of diuron transformation: a review. *Chemosphere* **2004**, *56*, 1021−1032.

(5) Field, J. A.; Reed, R. L.; Sawyer, T. E.; Martinez, M. Diuron and its metabolites in surface water and ground water by solid phase extraction and in-vial elution. *J. Agric. Food Chem.* **1997**, *45*, 3897−3902.
(6) Tixier, C.; Bogaerts, P.; Sancelme, M.; Bonnemoy, F.; Twagilimana, L.; Cuer, A.; Bohatier, J.; Veschambre, H. Fungal biodegradation of a phenylurea herbicide, diuron: structure and toxicity of metabolites. *Pest Manag. Sci.* **2000**, *56*, 455−462.
(7) Teisseire, H.; Couderchet, M.; Vernet, G. Phytotoxicity of diuron alone and in combination with copper or folpet on duckweed (*Lemna minor*). *Environ. Pollut.* **1999**, *106*, 39−45.
(8) Tlili, A.; Dorigo, U.; Montuelle, B.; Margoum, C.; Carluer, N.; Gouy, V.; Bouchez, A.; Bérard, A. Responses of chronically contaminated biofilms to short pulses of diuron. An experimental study simulating flooding events in a small river. *Aquat. Toxicol.* **2008**, *87*, 252−263.
(9) Chauhan, L. K. S.; Saxena, P. N.; Sundararaman, V.; Gupta, S. K. Diuron-induced cytological and ultrastructural alterations in the root meristem cells of *Allium cepa*. *Pestic. Biochem. Physiol.* **1998**, *62*, 152−163.
(10) Lambright, C.; Ostby, J.; Bobseine, K.; Wilson, V.; Hotchkiss, A. K.; Mann, P. C.; Gray, L. E., Jr. Cellular and molecular mechanisms of action of linuron: an antiandrogenic herbicide that produces reproductive malformations in male rats. *Toxicol. Sci.* **2000**, *56*, 389−399.
(11) Valentovic, M. A.; Yahia, T.; Ball, J. G.; Hong, S. K.; Brown, P. I.; Rankin, G. O. 3,4-Dichloroaniline acute toxicity in male Fisher 344 rats. *Toxicology* **1997**, *124*, 125−134.
(12) Werck-Reichhart, D.; Hehn, A.; Didierjean, L. Cytochromes P450 for engineering herbicide tolerance. *Trends Plant Sci.* **2000**, *5*, 116−123.
(13) Guzella, L.; Capri, E.; Di Corcia, A.; Barra Caracciolo, A.; Giuliano, G. Fate of diuron and linuron in a field lysimeter experiment. *J. Environ. Qual.* **2006**, *35*, 312−323.
(14) Breugelmans, P.; D'Huys, P.-J.; De Mot, R.; Springael, D. Characterization of novel linuron-mineralizing bacterial consortia enriched from long-term linuron-treated agricultural soils. *FEMS Microbiol. Ecol.* **2007**, *62*, 374−385.
(15) Anfossi, P.; Roncada, P.; Stracciari, G. L.; Montana, M.; Pasqualucci, C.; Montesissa, C. Toxicokinetics and metabolism of linuron in rabbit: *in vivo* and *in vitro* studies. *Xenobiotica* **1993**, *23*, 1113−1123.
(16) Frear, D. S.; Swanson, H. R.; Tanaka, F. S. N-demethylation of substituted 3-(phenyl)-1-methylureas: isolation and characterization of a microsomal mixed function oxidase from cotton. *Phytochemistry* **1969**, *8*, 2157−2169.
(17) Suzuki, T.; Casida, J. E. Metabolites of diuron, linuron, and methazole formed by liver microsomal enzymes and spinach plants. *J. Agric. Food Chem.* **1981**, *29*, 1027−1033.
(18) Pflugmacher, S.; Sandermann, H., Jr. Taxonomic distribution of plant glucosyltansferases acting on xenobiotics. *Phytochemistry* **1998**, *49*, 507−511.
(19) Meβner, B.; Thulke, O.; Schäffner, A. R. Arabidopsis glucosyltransferases with activities toward both endogenous and xenobiotic substrates. *Planta* **2003**, *217*, 138−146.
(20) Gachon, C. M. M.; Langlois-Meurinne, M.; Saindrenan, P. Plant secondary metabolism glycosyltransferases: the emerging functional analysis. *Trends Plant Sci.* **2005**, *10*, 542−549.
(21) Hollman, P. C. H.; van Trijp, J. M. P.; Buysman, N. C. P.; van der Gaag, M. S.; Mengelers, M. J. B.; de Vries, J. H. M.; Katan, M. B. Relative bioavailability of the antioxidant flavonoid quercetin from various foods in man. *FEBS Lett.* **1997**, *418*, 152−156.
(22) Karakaya, S. Bioavailability of phenolic compounds. *Crit. Rev. Food Sci. Nutr.* **2004**, *44*, 453−464.
(23) Manach, C.; Donovan, J. L. Pharmacokinetics and metabolism of dietary flavonoids in humans. *Free Radical Res.* **2004**, *38*, 771−785.
(24) Briggs, G. G.; Bromilow, R. H.; Evans, A. A. Relationship between lipophilicity and root uptake and translocation of non-ionised chemicals by barley. *Pestic. Sci.* **1982**, *13*, 495−504.
(25) De Carvalho, R. F.; Bromilow, R. H.; Greenwood, R. Uptake and translocation on non-ionised pesticides in the emergent aquatic plant parrot feather *Myriophyllum aquaticum*. *Pest Manag. Sci.* **2007**, *63*, 789−797.
(26) Salvestrini, S.; Di Cerbo, P.; Capasso, S. Kinetics and mechanism of hydrolysis of phenylureas. *J. Chem. Soc., Perkin Trans. 2* **2002**, 1889−1893.
(27) Shimabukuro, R. H.; Walsch, W. C. Xenobiotic metabolism in plants. In vitro, organ, and isolated cell techniques. In *Xenobiotic Metabolism: In Vitro Methods*; Paulson, G. D., Frear, D. S., Marks, E. P., Eds.; ACS Symposium Series; American Chemical Society: Washington, DC, 1979; Vol. 97, pp 3−34.
(28) Pascal-Lorber, S.; Rathahao, E.; Cravedi, J.-P.; Laurent, F. Uptake and metabolic fate of [^{14}C]-2,4-dichlorophenol and [^{14}C]-2,4-dichloroaniline in wheat (*Triticum aestivum*) and soybean (*Glycine max*). *J. Agric. Food Chem.* **2003**, *51*, 4712−4718.
(29) Walker, A.; Featherstone, R. M. Absorption and translocation of atrazine and linuron by plants with implications concerning linuron selectivity. *J. Exp. Bot.* **1973**, *24*, 450−458.
(30) Roberts, T. R. Nonextractable pesticide residues in soils and plants. *Pure Appl. Chem.* **1984**, *56*, 945−956.
(31) Bockers, M.; Rivero, C.; Thiede, B.; Jankowski, T.; Schmidt, B. Uptake, translocation, and metabolism of 3,4-dichloroaniline in soybean and wheat plants. *Z. Naturforsch.* **1994**, *49c*, 719−726.
(32) Pascal-Lorber, S.; Despoux, S.; Rathahao, E.; Canlet, C.; Debrauwer, L.; Laurent, F. Metabolic fate of [^{14}C] chlorophenols in radish (*Raphanus sativus*), lettuce (*Lactuca sativa*), and spinach (*Spinacia oleracea*). *J. Agric. Food Chem.* **2008**, *56*, 8461−8469.
(33) Brazier-Hicks, M.; Edwards, L. A.; Edwards, R. Selection of plants for roles in phytoremediation: the importance of glucosylation. *Plant Biotechnol. J.* **2007**, *5*, 627−635.
(34) Ortiz de Montellano, P. R. Oxygen activation and transfer. In *Cytochrome P-450: structure, mechanism and biochemistry*; Ortiz de Montellano, P. R., Ed.; Plenum Press: New York, London, 1986; pp 217−271.
(35) Cole, D. J.; Edwards, R. Secondary metabolism of agrochemicals in plants. In *Metabolism of Agrochemicals in Plants*; Robert, T., Ed.; John Wiley & Sons Ltd: Chichester, U.K., 2000; pp 107−154.
(36) Loutre, C.; Dixon, D. P.; Brazier, M.; Slater, M.; Cole, D. J.; Edwards, R. Isolation of a glucosyltransferase from *Arabidopsis thaliana* active in the metabolism of the persistent pollutant 3,4-dichloroaniline. *Plant J.* **2003**, *34*, 485−493.
(37) Durst, F. Métabolisation des herbicides. In *Les herbicides, mode d'action et principes d'utilisation*; Scalla, R., Ed.; INRA: Paris, France, 1991; pp 193−236.
(38) Brazier-Hicks, M.; Evans, K. M.; Gershater, M. C.; Puschmann, H.; Steel, P. G.; Edwards, R. C-Glycosylation of flavonoids in cereals. *J. Biol. Chem.* **2009**, *284*, 17926−17934.
(39) Viskupičová, J.; Ondrejovič, M.; Šturdík, E. Bioavailability and metabolism of flavonoids. *J. Food Nutr. Res.* **2008**, *4*, 151−162.